Low-Complexity Gridless 2D Harmonic Retrieval via Decoupled-ANM Covariance Reconstruction

Yu Zhang[†*], Yue Wang[*], Zhi Tian[*], Geert Leus[‡], Gong Zhang[†]

[†]*College of EIE, Nanjing University of Aeronautics and Astronautics, Nanjing, China*

[*]*Department of ECE, George Mason University, Fairfax, VA, USA*

[‡]*Faculty of EEMCS, Delft University of Technology, Delft, The Netherlands*

Emails: {skywalker_zy, gzhang}@nuaa.edu.cn, {ywang56, ztian1}@gmu.edu, g.j.t.leus@tudelft.nl

***Abstract*—This paper aims at developing low-complexity solutions for super-resolution two-dimensional (2D) harmonic retrieval via covariance reconstruction. Given the collected sample covariance, a novel gridless compressed sensing approach is designed based on the atomic norm minimization (ANM) technique. The key is to perform a redundancy reduction (RR) transformation that effectively reduces the large problem size at hand, without loss of useful frequency information. For uncorrelated sources, the transformed 2D covariance matrices in the RR domain retain a salient structure, which permits a sparse representation over a matrix-form atom set with decoupled 1D frequency components. Accordingly, the decoupled ANM (D-ANM) framework can be applied for super-resolution 2D frequency estimation, at low computational complexity on the same order of the 1D case. An analysis of the complexity reduction of the proposed RR-D-ANM compared with benchmark methods is provided as well, which is verified by our simulation results.**

***Index Terms*—Low complexity, 2D harmonic retrieval, covariance reconstruction, D-ANM, RR transformation,**

I. INTRODUCTION

Two-dimensional (2D) harmonic retrieval has broad applications, e.g., speech processing [1], wireless communications [2], radar systems [3], etc. In the case of multiple measurement vectors (MMV), a number of high-resolution covariance-based methods have been proposed, with computational complexities that are independent of the number of MMV. However, classical covariance-based methods based on a statistical analysis of the sample covariance [4]–[7], may not work well for applications with limited sampling resources, such as, short sensing time and compressive measurements. Although methods based on compressive sensing (CS) techniques can address these issues [8]–[11], they critically rely on an on-grid assumption and hence suffer from the basis mismatch problem [12].

Recently, to overcome this problem, two super-resolution gridless CS approaches are proposed for the MMV case based on low-rank structured covariance reconstruction (LRSCR) [13] and vectorization-based atomic norm minimization (V-ANM) [14], [15], respectively. Unfortunately, the computational complexities of both techniques scale exponentially with the dimensionality, and will become unacceptable for practical implementations. In contrast, the decoupled ANM (D-ANM) [16], [17], by virtue of its frequency decoupling strategy, effectively reduces the computational complexity to be comparable to that of a 1D ANM solution, at no loss of optimality [18]. However, the D-ANM only applies to the single measurement vector (SMV) case. To the best of our knowledge, there is still a lack of computationally efficient covariance-based gridless 2D harmonic retrieval techniques.

To fill this gap, by exploiting the structural information of the sample covariance matrix, we propose a novel covariance-based gridless method for 2D harmonic retrieval with low computational complexity, termed redundancy-reduction (RR) transformation based D-ANM (RR-D-ANM). Specifically, given the inherent two-level Toeplitz structure of the covariance matrix in the uncorrelated case, we propose an RR transformation to concisely express the vectorized covariance matrix as an RR vector via a linear projection. Then, by exploiting the sparsity of the RR vector which can be sparsely represented by a decoupled atom set, we propose an efficient gridless 2D harmonic retrieval solution via RR-enabled D-ANM with MMV. Further, to make the problem tractable, we equivalently reformulate the original formulation as a solvable convex form based on the uniqueness of the existence of the generalized Vandermonde decomposition of the covariance matrix. Simulation results verify the advantages of the proposed RR-D-ANM in terms of reduced complexity at no significant loss of performance.

Notations: a, $\boldsymbol{a}$, $\boldsymbol{A}$ and $\mathcal{A}$ denote a scalar, a vector, a matrix, and a atom set, respectively. $(\cdot)^T$, $(\cdot)^*$, and $(\cdot)^H$ are the transpose, conjugate, and conjugate transpose operation, respectively. $\|\boldsymbol{a}\|_1$ and $\|\boldsymbol{a}\|_2$ denote the ℓ_1 and ℓ_2 norm of $\boldsymbol{a}$, respectively. $\text{diag}(\boldsymbol{a})$ generates a diagonal matrix with the diagonal elements constructed from $\boldsymbol{a}$. $\text{T}(\boldsymbol{a})$ is a Hermitian Toeplitz matrix with first column being $\boldsymbol{a}$. $\text{Tr}(\boldsymbol{A})$ is the trace of $\boldsymbol{A}$. $\boldsymbol{I}$ denotes the identity matrix. The operation $\text{vec}(\cdot)$ stacks all the columns of a matrix into a vector and $\text{vec}^{-1}(\cdot)$ is the inverse operation of $\text{vec}(\cdot)$. $\mathbb{E}\{\cdot\}$ denotes expectation. $\otimes$ calculates the Kronecker product of matrices or vectors. $\odot$ computes the Khatri-Rao product of matrices.

II. SIGNAL MODEL

Consider a 2D harmonic retrieval problem where the signal of interest $\boldsymbol{x}(t) \in \mathbb{C}^{NM\times 1}$ is a linear mixture of K 2D

This work was supported in part by the US National Science Foundation grants #1527396 and #1547364, and the National Science Foundation of China grants #61871218, #61801211 and #61471191. This work was partly carried out in the frame of the ASPIRE project (project 14926 within the OTP program of NWO-TTW).

sinusoidal components in the form of

$$\begin{aligned}\boldsymbol{x}(t) &= \sum_{i=1}^{K} s_i(t)\left[\boldsymbol{a}_N(f_{1,i}) \otimes \boldsymbol{a}_M(f_{2,i})\right] = \sum_{i=1}^{K} s_i(t)\boldsymbol{a}_{2D}(\boldsymbol{f}^i) \\ &= (\boldsymbol{A}_N \odot \boldsymbol{A}_M)\boldsymbol{s}(t), \qquad t = 1,\dots,L, \end{aligned} \tag{1}$$

where $s_i(t)$ is the complex amplitude of the i-th source, $\boldsymbol{f}^i = (f_{1,i}, f_{2,i})^T \in [-0.5, 0.5)^2$ consists of its digital frequencies along the two orthogonal dimensions, and L is the number of measurement vectors. The 2D manifold vector $\boldsymbol{a}_{2D}(\boldsymbol{f}^i) = \boldsymbol{a}_N(f_{1,i}) \otimes \boldsymbol{a}_M(f_{2,i})$ is composed of two Vandermonde-structured manifold vectors $\boldsymbol{a}_N(f_{1,i})$ and $\boldsymbol{a}_M(f_{2,i})$ of size N and M respectively, of the form[1]

$$\begin{aligned}\boldsymbol{a}_N(f_{1,i}) &= [1, \exp(j2\pi f_{1,i}), \dots, \exp(j2\pi(N-1)f_{1,i})]^T, \\ \boldsymbol{a}_M(f_{2,i}) &= [1, \exp(j2\pi f_{2,i}), \dots, \exp(j2\pi(M-1)f_{2,i})]^T. \end{aligned} \tag{2}$$

Further, $\boldsymbol{s}(t) = [s_1(t), \dots, s_K(t)]^T$, $\boldsymbol{f}_n = [f_{n,1}, \dots, f_{n,K}]$ for $n = 1, 2$, $\boldsymbol{A}_N = \boldsymbol{A}_N(\boldsymbol{f}_1) = [\boldsymbol{a}_N(f_{1,1}), \dots, \boldsymbol{a}_N(f_{1,K})]$, and $\boldsymbol{A}_M = \boldsymbol{A}_M(\boldsymbol{f}_2) = [\boldsymbol{a}_M(f_{2,1}), \dots, \boldsymbol{a}_M(f_{2,K})]$.

In many applications, $\boldsymbol{x}(t)$ is not observed directly, but through subsampling or linear compression via a measurement matrix $\boldsymbol{J} \in \mathbb{C}^{M' \times NM}$ with $M' \le NM$. Inflicted by an additive Gaussian noise $\boldsymbol{n}(t)$, the SMV $\boldsymbol{y}(t) \in \mathbb{C}^{M'}$ is given by $\boldsymbol{y}(t) = \boldsymbol{J}\boldsymbol{x}(t) + \boldsymbol{n}(t)$. Given random $\boldsymbol{s}(t)$, the desired frequency information lies in the covariance of $\boldsymbol{y}(t)$, defined by

$$\boldsymbol{R}_y = \mathbb{E}\{\boldsymbol{y}(t)\boldsymbol{y}(t)^H\} = \boldsymbol{J}\boldsymbol{R}_x\boldsymbol{J}^H + \boldsymbol{R}_n, \tag{3}$$

where $\boldsymbol{R}_x$ and $\boldsymbol{R}_n$ are the covariance of $\boldsymbol{x}(t)$ and $\boldsymbol{n}(t)$, respectively. Denoting $\boldsymbol{R}_s = \mathbb{E}\{\boldsymbol{s}(t)\boldsymbol{s}(t)^H\}$, we have

$$\boldsymbol{R}_x = \mathbb{E}\{\boldsymbol{x}(t)\boldsymbol{x}(t)^H\} = (\boldsymbol{A}_N \odot \boldsymbol{A}_M)\boldsymbol{R}_s(\boldsymbol{A}_N \odot \boldsymbol{A}_M)^H. \tag{4}$$

This paper considers uncorrelated signal sources, that is, $\mathbb{E}\{s_i(t)s_j^*(t)\} = r_i\delta_{ij}$, $\forall 1 \le i, j \le K$. Since $r_i \ge 0$, $\forall i$, $\boldsymbol{R}_s$ is a positive semidefinite (PSD) diagonal matrix:

$$\boldsymbol{R}_s = \mathrm{diag}(\boldsymbol{r}) \succeq 0, \quad \text{where } \boldsymbol{r} = [r_1, \dots, r_K]^T. \tag{5}$$

In practice, $\boldsymbol{R}_y$ is approximated by its sample covariance

$$\hat{\boldsymbol{R}}_y = \frac{1}{L}\sum_{t=1}^{L} \boldsymbol{y}(t)\boldsymbol{y}^H(t). \tag{6}$$

The goal of the 2D harmonic retrieval in this paper is to recover the unknown frequency pairs $\{\boldsymbol{f}^i\}_i$ from $\hat{\boldsymbol{R}}_y$.

III. Redundancy-reduction based D-ANM for Harmonic Retrieval

This section develops a super-resolution 2D frequency estimation scheme based on the D-ANM scheme, in the presence of MMV case. A redundancy-reduction transformation of the signal covariance is introduced, which effectively reduces the computational cost to be comparable to that of a 1D problem.

[1] In this paper, we mainly focus on uniform sampling scenarios. When non-ideal geometries are encountered, for example antenna systems with perturbation due to array mismatch, array manifold separation techniques can be applied to retrieve the Vandermonde structure through a Bessel or Fourier approximation [19], [20].

A. Redundancy-reduction Transformation

To take advantage of the low complexity of the D-ANM which can only be employed for the SMV case, we turn to $\boldsymbol{r}_x = \mathrm{vec}(\boldsymbol{R}_x) \in \mathbb{C}^{(NM)^2}$ as the structured signal vector of interest. This single vector can be approximated by $\mathrm{vec}\left(\frac{1}{L}\sum_{t=1}^{L}\boldsymbol{x}(t)\boldsymbol{x}^H(t)\right)$, which retains the useful frequency information of all $\{\boldsymbol{x}(t)\}_t$. Hence, an MMV problem based on $\{\boldsymbol{x}(t)\}_t$ can be alternatively solved as an SMV problem based on $\boldsymbol{r}_x$, which makes it amenable to the D-ANM scheme.

However, the benefit of adopting $\boldsymbol{r}_x$ as the signal of interest comes at the expense of a much enlarged signal length of $(NM)^2$, which may incur a high computational cost. To circumvent this issue, we propose a RR transformation to concisely express $\boldsymbol{r}_x$, by removing the redundancy in the entries of $\boldsymbol{r}_x$. The basic idea is to establish a linear mapping that projects the vectorized covariance matrix $\boldsymbol{r}_x$ with repeated entries onto an RR vector $\boldsymbol{z}$ with no repeated entries. A similar thought can be found in our previous work where we establish a the linear mapping between the covariance matrices in the compressed and uncompressed domains for compressive cyclic feature detection [21], [22] and DOA estimation [23].

The inherent redundancy in $\boldsymbol{r}_x$ is due to the uncorrelated sources, which yields $\boldsymbol{R}_s = \mathrm{diag}(\boldsymbol{r})$ with only K nonzero entries. By vectorizing both sides of (4), it follows that

$$\boldsymbol{r}_x = \sum_{i=1}^{K} r_i \left(\boldsymbol{a}_N(f_{1,i}) \otimes \boldsymbol{a}_M(f_{2,i})\right)^* \otimes \left(\boldsymbol{a}_N(f_{1,i}) \otimes \boldsymbol{a}_M(f_{2,i})\right). \tag{7}$$

Concerning each summand in (7), an important equality arises:

$$\begin{aligned}&\left(\boldsymbol{a}_N(f_{1,i}) \otimes \boldsymbol{a}_M(f_{2,i})\right)^* \otimes \left(\boldsymbol{a}_N(f_{1,i}) \otimes \boldsymbol{a}_M(f_{2,i})\right) \\ &= \boldsymbol{\Psi}(\boldsymbol{a}'_N(f_{1,i}) \otimes \boldsymbol{a}'_M(f_{2,i})), \end{aligned} \tag{8}$$

where $\boldsymbol{a}'_N(f_{1,i}) \in \mathbb{C}^{2N-1}$ and $\boldsymbol{a}'_M(f_{2,i}) \in \mathbb{C}^{2M-1}$ are given by

$$\begin{aligned}&\boldsymbol{a}'_N(f_{1,i}) \\ &= [e^{-j2\pi(N-1)f_{1,i}}, \dots, e^{-j2\pi f_{1,i}}, 1, e^{j2\pi f_{1,i}}, \dots, e^{j2\pi(N-1)f_{1,i}}]^T, \\ &\boldsymbol{a}'_M(f_{2,i}) \\ &= [e^{-j2\pi(M-1)f_{2,i}}, \dots, e^{-j2\pi f_{2,i}}, 1, e^{j2\pi f_{2,i}}, \dots, e^{j2\pi(M-1)f_{2,i}}]^T. \end{aligned} \tag{9}$$

The matrix $\boldsymbol{\Psi} = (\boldsymbol{I}_N \otimes \boldsymbol{E} \otimes \boldsymbol{I}_M)(\boldsymbol{G}_N \otimes \boldsymbol{G}_M)$ is the redundancy-reduction (RR) transformation matrix that is determined by N and M only, where $\boldsymbol{E} = \sum_{j=1}^{M}(\boldsymbol{e}_j^T \otimes \boldsymbol{I}_N \otimes \boldsymbol{e}_j) \in \mathbb{C}^{NM \times NM}$ is the commutation matrix, $\boldsymbol{G}_N$ is defined as

$$\boldsymbol{G}_N = \left[\boldsymbol{G}_{N,1}^T, \dots, \boldsymbol{G}_{N,N}^T\right]^T \in \mathbb{C}^{N^2 \times (2N-1)}, \tag{10}$$

with the i-th block matrix $\boldsymbol{G}_{N,i} = [\boldsymbol{0}_{N \times (N-i)}, \boldsymbol{I}_N, \boldsymbol{0}_{N \times (i-1)}]$, $i = 1, \dots, N$, and $\boldsymbol{G}_M \in \mathbb{C}^{M^2 \times (2M-1)}$ is defined similarly as (10).

Defining $\boldsymbol{a}'_{2D}(\boldsymbol{f}) = \boldsymbol{a}'_N(f_1) \otimes \boldsymbol{a}'_M(f_2)$, we have

$$\boldsymbol{r}_x = \boldsymbol{\Psi}\boldsymbol{z}, \quad \text{with } \boldsymbol{z} = \sum_{i=1}^{K} r_i \boldsymbol{a}'_{2D}(\boldsymbol{f}^i) = (\boldsymbol{A}'_N \odot \boldsymbol{A}'_M)\boldsymbol{r}, \tag{11}$$

where $\boldsymbol{A}'_N = \boldsymbol{A}'_N(\boldsymbol{f}_1) = [\boldsymbol{a}'_N(f_{1,1}), \ldots, \boldsymbol{a}'_N(f_{1,K})]$ and $\boldsymbol{A}'_M = \boldsymbol{A}'_M(\boldsymbol{f}_2) = [\boldsymbol{a}'_M(f_{2,1}), \ldots, \boldsymbol{a}'_M(f_{2,K})]$. Moreover, we have

$$\boldsymbol{z} = \text{vec}(\boldsymbol{A}'_M \boldsymbol{R}_s \boldsymbol{A}'^T_N) = \text{vec}(\boldsymbol{Z}), \tag{12}$$

where $\boldsymbol{Z} = \boldsymbol{A}'_M \boldsymbol{R}_s \boldsymbol{A}'^T_N$.

Apparently, $\boldsymbol{z}$ in (12) can be observed through $\boldsymbol{r}_y$ by noting

$$\begin{aligned} \boldsymbol{r}_y = \text{vec}(\boldsymbol{R}_y) &= \text{vec}(\boldsymbol{J}\boldsymbol{R}_x\boldsymbol{J}^H + \boldsymbol{R}_n) \\ &= (\boldsymbol{J}^* \otimes \boldsymbol{J})\boldsymbol{\Psi}\boldsymbol{z} + \boldsymbol{r}_n = \boldsymbol{\Gamma}\boldsymbol{z} + \boldsymbol{r}_n, \end{aligned} \tag{13}$$

where $\boldsymbol{\Gamma} = (\boldsymbol{J}^* \otimes \boldsymbol{J})\boldsymbol{\Psi} \in \mathbb{C}^{M'^2 \times c}$ with $c = (2N-1)(2M-1)$, and $\boldsymbol{r}_n = \text{vec}(\boldsymbol{R}_n)$ is the noise term.

It is worth noting the importance of (11) and (13) as the equivalent signal and measurement models in the RR domain. Noticeably, the RR vector $\boldsymbol{z}$, or its matrix form $\boldsymbol{Z}$, contains all the harmonic information. It is the RR transformation matrix $\boldsymbol{\Psi}$ that linearly maps the original $\boldsymbol{r}_x$ of a large size N^2M^2 to a much smaller vector $\boldsymbol{z}$ of size $(2N-1)(2M-1)$, without loss of any useful information. More importantly, the dimensionality is reduced as well. As indicated in (8), $\boldsymbol{r}_x$ in the original domain is structurally complex consisting of four nested Vandermonde vectors, which is difficult to tackle. In contract, the RR vector $\boldsymbol{z}$ is modeled to retain the two-level Vandermonde structure in its manifold vector $\boldsymbol{a}'_{_{2D}}(\boldsymbol{f}^i)$, parameterized by the unknown frequencies of interest. Note that $\hat{\boldsymbol{r}}_y = \text{vec}(\hat{\boldsymbol{R}}_y)$ is linearly related to the RR vector $\boldsymbol{z}$ with (13). Now, the task boils down to reconstructing the 2D structure of $\boldsymbol{z}$ or $\boldsymbol{Z}$ in the RR domain from $\hat{\boldsymbol{r}}_y$, which is presented next.

B. Harmonic Retrieval via D-ANM

In the RR domain, the model of $\boldsymbol{z}$ in (11) bears a similar form as that of $\boldsymbol{x}$ in (1). An intricate difference is that the coefficients $\boldsymbol{r} = [r_1, \ldots, r_K]^T$ in $\boldsymbol{z}$ are nonnegative, whereas $\boldsymbol{x}$ has complex-valued coefficients. Since all the gridless CS techniques for the simple SMV case, including the V-ANM and D-ANM, can be applied with the measurement $\boldsymbol{y}(t)$ to retrieval $\boldsymbol{x}(t)$, these techniques can be applied for $\boldsymbol{z}$ reconstruction, only with an extra care on the nonnegativeness of $\boldsymbol{r}$.

Considering the computational efficiency of D-ANM over V-ANM, we aim to develop a D-ANM solution to extract the structural information of the RR vector $\boldsymbol{z}$. To this end, we inspect its matrix form $\boldsymbol{Z}$ in (12):

$$\boldsymbol{Z} = \text{vec}^{-1}(\boldsymbol{z}) = \sum_{i=1}^{K} r_i \boldsymbol{a}'_M(f_{2,i})\boldsymbol{a}'^T_N(f_{1,i}) = \sum_{i=1}^{K} r_i \boldsymbol{A}'(\boldsymbol{f}^i),$$

where $\boldsymbol{A}'(\boldsymbol{f}^i) = \boldsymbol{a}'_M(f_{2,i})\boldsymbol{a}'^T_N(f_{1,i})$. Apparently, $\boldsymbol{Z}$ has a sparse linear atomic representation over the following matrix-form atom set of infinite size:

$$\mathcal{A}'_d = \left\{ \boldsymbol{A}'(\boldsymbol{f}), \quad \forall \boldsymbol{f} \in (-\tfrac{1}{2}, \tfrac{1}{2}] \times (-\tfrac{1}{2}, \tfrac{1}{2}] \right\}. \tag{14}$$

We introduce a new matrix-form atomic norm

$$\begin{aligned} &\|\boldsymbol{Z}\|^+_{\mathcal{A}'_d} = \\ &\inf\left\{ \sum_k r_k \middle| \sum_k r_k \boldsymbol{A}'(\boldsymbol{f}^k), \quad \boldsymbol{A}'(\boldsymbol{f}^k) \in \mathcal{A}'_d; r_k \geq 0, \forall k \right\}, \end{aligned} \tag{15}$$

which differs from the standard D-ANM $\|\boldsymbol{Z}\|_{\mathcal{A}'_d}$ in [18], because of the extra constraint $\boldsymbol{r} \geq \boldsymbol{0}$.

Given $\boldsymbol{Z}$, it is possible to retrieve the components $\{r_k, \boldsymbol{f}^k\}$ of its sparest representation by calculating its atomic norm, which results in a line spectrum estimation. In the presence of noise, it boils down to

$$\widetilde{\boldsymbol{Z}} = \arg\min_{\boldsymbol{Z}} \|\boldsymbol{Z}\|^+_{\mathcal{A}'_d} \quad \text{s.t.} \quad \|\boldsymbol{r}_y - \boldsymbol{\Gamma}\text{vec}(\boldsymbol{Z})\|_2^2 \leq \beta, \tag{16}$$

where β indicates the noise tolerance threshold. To approach the standard D-ANM technique, we re-write (16) into the following equivalent form:

$$\min_{\boldsymbol{Z}(\boldsymbol{r}, \boldsymbol{f}_1, \boldsymbol{f}_2), \boldsymbol{r}} \quad \|\boldsymbol{Z}\|_{\mathcal{A}'_d} = \|\boldsymbol{r}\|_1 \tag{17a}$$

$$\text{s.t.} \quad \|\boldsymbol{r}_y - \boldsymbol{\Gamma}\text{vec}(\boldsymbol{Z})\|_2^2 \leq \beta \tag{17b}$$

$$\boldsymbol{Z} = \boldsymbol{A}'_M(\boldsymbol{f}_2)\text{diag}(\boldsymbol{r})\boldsymbol{A}'^T_N(\boldsymbol{f}_1) \tag{17c}$$

$$\boldsymbol{r} \geq \boldsymbol{0}. \tag{17d}$$

Here (17c) is implicit in the objective function of (16), but becomes an explicit constraint because of the new nonnegative constraint (17d). Without (17d), the semidefinite programming (SDP) implementation of the D-ANM proposed in [18] can be used to reformulate (17) into a convex problem. However, because of the extra constraint on $\boldsymbol{r}$ in (17d), this problem becomes intractable, because $\boldsymbol{r}$ is intertwined with the other variable $\boldsymbol{Z}$ in the form of (17c).

To solve (17) in a tractable manner, we seek to reformulate $\boldsymbol{r} \geq \boldsymbol{0}$ to an equivalent form with respect to $\boldsymbol{Z}$. To this end, we note that $\boldsymbol{Z} = \text{vec}^{-1}(\boldsymbol{z})$ in the RR domain is linearly related to $\boldsymbol{R}_x = \text{vec}^{-1}(\boldsymbol{r}_x)$, via

$$\boldsymbol{R}_x = \text{vec}^{-1}(\boldsymbol{r}_x) = \text{vec}^{-1}(\boldsymbol{\Psi}\boldsymbol{z}) = \text{vec}^{-1}\left(\boldsymbol{\Psi}\text{vec}(\boldsymbol{Z})\right). \tag{18}$$

When there exists a unique generalized Vandermonde decomposition of $\boldsymbol{R}_x$, it holds that $\boldsymbol{r} \geq \boldsymbol{0}$ if and only if $\boldsymbol{R}_x \succeq 0$. Fortunately, thanks to the specific structure of $\boldsymbol{Z}$ in (17c), the decomposition property of $\boldsymbol{R}_x$ represented in the form of (18) can be guaranteed. Moreover, $\boldsymbol{R}_x \succeq 0$ can be expressed by the following PSD constraint parameterized by $\boldsymbol{Z}$:

$$\text{vec}^{-1}\left(\boldsymbol{\Psi}\text{vec}(\boldsymbol{Z})\right) \succeq 0. \tag{19}$$

Adopting (19) to replace (17d), and reformulating (17a)-(17c) into the decoupled SDP form proposed in [18], we reach the following equivalent SDP problem for (16)[2] :

$$\{\widetilde{\boldsymbol{Z}}, \widetilde{\boldsymbol{u}}_N, \widetilde{\boldsymbol{u}}_M\} \tag{20a}$$

$$= \arg \min_{\substack{\boldsymbol{Z}, \boldsymbol{u}_N \\ \boldsymbol{u}_M}} \frac{1}{2\sqrt{c}} (\mathrm{Tr}(\mathrm{T}(\boldsymbol{u}_N)) + \mathrm{Tr}(\mathrm{T}(\boldsymbol{u}_M))) \tag{20b}$$

$$\text{s.t.} \quad \left\| \mathrm{vec}(\hat{\boldsymbol{R}}_y) - \boldsymbol{\Gamma} \mathrm{vec}(\boldsymbol{Z}) \right\|_2^2 \leq \beta, \tag{20c}$$

$$\begin{bmatrix} \mathrm{T}(\boldsymbol{u}_M) & \boldsymbol{Z} \\ \boldsymbol{Z}^H & \mathrm{T}(\boldsymbol{u}_N) \end{bmatrix} \succeq 0, \tag{20d}$$

$$\mathrm{vec}^{-1}(\boldsymbol{\Psi} \mathrm{vec}(\boldsymbol{Z})) \succeq 0. \tag{20e}$$

With the obtained $\widetilde{\boldsymbol{Z}}$, we can sequentially obtain the signal covariance matrix estimation $\widetilde{\boldsymbol{R}}_x$ from (18) and then, the Matrix Pencil and Pairing (MaPP) proposed in [14] can be employed for harmonic retrieval.

Remark 1: (20) is the SDP-based D-ANM solution for covariance reconstruction in the RR domain, which we term as RR-D-ANM. It lumps all the measurements $\{\boldsymbol{y}(t)\}_t$ into a single vector $\hat{\boldsymbol{r}}_y$ in order to decouple the frequency-dependent variables into 1D without loss of optimality. Because of this decoupling, the PSD matrix in (20d) is of size $2(2M-1) \times 2(2N-1)$. However, the extra PSD constraint in (20e) is of size $MN \times MN$, which raises the complexity order to be comparable to V-ANM [14] and LRSCR [13]. Fortunately, when L is reasonable large, this covariance-based constraint is mostly satisfied, and hence can be removed leading to a truncated version termed RR-D-ANM-w/o3, to balance the computational cost and performance. Simulation results verify this balance.

IV. Computational Complexity

According to Vandenberghe and Boyd [25], the computational complexity of solving our RR-D-ANM in (20) is $\mathcal{O}((NM)^{4.5})$, which remains the same as that of the LRSCR, due to their comparable problem scales dominated by the same largest-size PSD constraints. Fortunately, as claimed in *Remark* 1, since the strong structure of the covariance matrix is captured via D-ANM, the largest PSD constraint of (20e) can be omitted to balance the computational cost and performance. Accordingly, with the remaining smaller-size PSD constraint of (20d), the complexity of the resulting RR-D-ANM-w/o3 drops down to $\mathcal{O}((NM)^2(N+M)^{2.5})$, which is 2.5 orders lower than that of the RR-D-ANM, as well as the LRSCR, when $N = M$. Moreover, to further reduce the computational complexity, the proposed method can be fast implemented via the alternating direction method of multipliers (ADMM) technique [26].

V. Simulation Results

This section presents numerical results to evaluate the performance and the complexity of the RR-D-ANM solutions, while the LRSCR [13], the conventional MUSIC algorithm [4] and the CRB for full observation [27] are considered as benchmark. All simulations run on a computer with a 4-core Intel i7-6500U 2.60GHz CPU and 8GB memory. The root mean squared error (RMSE) is measured to evaluate the estimation accuracy of 2D harmonic retrieval as RMSE $= \frac{1}{K}\sum_{i=1}^{K}\Big(\frac{1}{M_t}\sum_{n=1}^{M_t}\Big((\widetilde{f}_{1,i}^n - f_{1,i})^2 + (\widetilde{f}_{2,i}^n - f_{2,i})^2\Big)\Big)^{\frac{1}{2}}$, where M_t, $\widetilde{f}_{1,i}^n$ and $\widetilde{f}_{2,i}^n$ denote the number of Monte-Carlo trials, and the estimates of $f_{1,i}$ and $f_{2,i}$ in the n-th trial, respectively. In the simulations, the noise is considered as Gaussian white noise satisfying $\boldsymbol{n}(t) \sim (\boldsymbol{0}, \sigma^2\boldsymbol{I})$, the measurement matrix $\boldsymbol{J}$ is randomly generated, and then, the user-specified parameter β is determined via the covariance matrix fitting criterion [23].

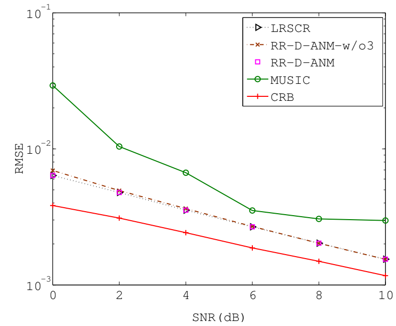

(a) RMSE vs. SNR with L=200

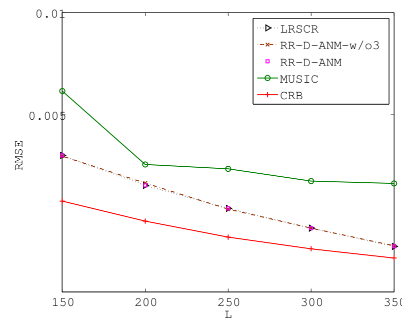

(b) RMSE vs. L with SNR=5dB

Fig. 1: Estimation accuracy for RR-D-ANM, RR-D-ANM-w/o3, LRSCR, MUSIC and CRB, when $M = N = 5$, $M' = 15$ and $K = 3$.

We first evaluate the estimation performance of the proposed methods. For a fair comparison, all methods incorporate with the MaPP for harmonic retrieval. As shown in Fig. 1, the conventional MUSIC can not achieve a desired performance under the randomly compressed scenario. The proposed RR-D-ANM obtains the same performance as that of the benchmark LRSCR. While the proposed RR-D-ANM slightly outperforms the RR-D-ANM-w/o3, the gap between them becomes small and diminishes as the SNR or the number of measurement vectors increase. Moreover, the simulation results indicate that the performance gap within the whole evaluation range is less than 10^{-3}, which means such a performance loss is negligible.

Further, the computational complexity is tested and com-

[2]In this paper, we consider sufficient separated frequencies to match the minimum frequenc separation requirement [18]. Moreover, the reweighted ANM technique inspired by [24] can be utilized to enhance sparsity and resolution when unknown frequencies are spaced closely.

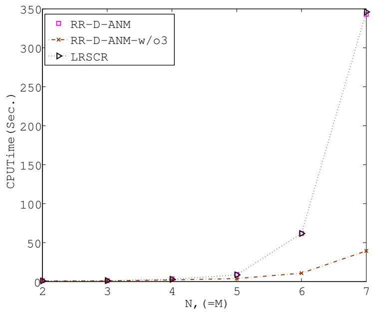

Fig. 2: Computational complexity of RR-D-ANM, RR-D-ANM-w/o3 and LRSCR in terms of runtime with $L = 200$, SNR $= 10$dB and $M' = \lfloor \frac{NM}{2} \rfloor + 1$.

pared, where all methods use the off-the-shelf SDP-based solver [28]. As shown in Fig. 2, the complexity of the proposed RR-D-ANM remains the same order as that of the LRSCR. On the other hand, the complexity of the RR-D-ANM-w/o3 is reduced dramatically. In this sense, the RR-D-ANM-w/o3 can achieve huge computational savings with a negligible performance loss compared with the RR-D-ANM and the LRSCR. Therefore, it provides an excellent tradeoff to balance the performance and the complexity for 2D harmonic retrieval, especially when N and/or M go large.

VI. Conclusion

In this paper, we proposed a gridless compressed sensing framework based on the D-ANM technique, to efficiently perform super-resolution 2D harmonic estimation with the sample covariance collected from MMV. Specifically, we first established an RR transformation to linearly map the originally large-size covariance matrix to a small-size RR vector. Then, the sparse representation of the transformed RR vector enables to reformulate the originally complex 2D MMV harmonic retrieval problem as an RR-based D-ANM problem, which can be resolved efficiently at a much reduced computational complexity. Simulation results demonstrate such an advantage of our solutions over the existing ones.

References

[1] J. C. J. Benesty and Y. Huang, *Microphone Array Signal Processing*. New York, NY, USA: Springer, 2008, vol. 1.

[2] Y. Wang, P. Xu, and Z. Tian, “Efficient channel estimation for massive MIMO systems via truncated two-dimensional atomic norm minimization,” in *Proc. IEEE Int. Conf. Communications (ICC)*, May 2017, pp. 1–6.

[3] F. Wen, X. Xiong, and Z. Zhang, “Angle and mutual coupling estimation in bistatic mimo radar based on parafac decomposition,” *Digital Signal Processing*, vol. 65, pp. 1–10, 2017.

[4] R. Schmidt, “Multiple emitter location and signal parameter estimation,” *IEEE transactions on antennas and propagation*, vol. 34, no. 3, pp. 276–280, 1986.

[5] J. Li and R. T. Compton, “Two-dimensional angle and polarization estimation using the ESPRIT algorithm,” *IEEE Transactions on Antennas and Propagation*, vol. 40, no. 5, pp. 550–555, May 1992.

[6] M. A. Doron and E. Doron, “Wavefield modeling and array processing. ii. algorithms,” *IEEE Transactions on Signal Processing*, vol. 42, no. 10, pp. 2560 – 2570, Oct. 1994.

[7] M. Haardt, M. Zoltowski, C. Mathews, and J. Nossek, “2d unitary esprit for efficient 2d parameter estimation,” in *ICASSP’84. IEEE International Conference on Acoustics, Speech, and Signal Processing*. IEEE, 1995.

[8] P. Stoica, P. Babu, and J. Li, “Spice: A sparse covariance-based estimation method for array processing,” *IEEE Transactions on Signal Processing*, vol. 59, no. 2, pp. 629–638, Feb. 2011.

[9] Z. Liu, Z. Huang, and Y. Zhou, “Array signal processing via sparsity-inducing representation of the array covariance matrix,” *IEEE Transactions on Aerospace and Electronic Systems*, vol. 49, no. 3, pp. 1710–1724, Jul. 2013.

[10] Y. Wang, Z. Tian, S. Feng, and P. Zhang, “Efficient channel statistics estimation for millimeter-wave MIMO systems,” in *Proc. Speech and Signal Processing (ICASSP) 2016 IEEE Int. Conf. Acoustics*, Mar. 2016, pp. 3411–3415.

[11] ——, “A fast channel estimation approach for millimeter-wave massive MIMO systems,” in *Proc. IEEE Global Conf. Signal and Information Processing (GlobalSIP)*, Dec. 2016, pp. 1413–1417.

[12] Y. Chi, L. L. Scharf, A. Pezeshki, and A. R. Calderbank, “Sensitivity to basis mismatch in compressed sensing,” *IEEE Transactions on Signal Processing*, vol. 59, no. 5, pp. 2182–2195, May 2011.

[13] X. Tian, J. Lei, and L. Du, “A generalized 2-D DOA estimation method based on low-rank matrix reconstruction,” *IEEE Access*, vol. 6, pp. 17 407–17 414, 2018.

[14] Z. Yang, L. Xie, and P. Stoica, “Vandermonde decomposition of multilevel Toeplitz matrices with application to multidimensional super-resolution,” *IEEE Transactions on Information Theory*, vol. 62, no. 6, pp. 3685–3701, Jun. 2016.

[15] J. Steinwandt, F. Roemer, C. Steffens, M. Haardt, and M. Pesavento, “Gridless super-resolution direction finding for strictly non-circular sources based on atomic norm minimization,” in *Proc. Systems and Computers 2016 50th Asilomar Conf. Signals*, Nov. 2016, pp. 1518–1522.

[16] Z. Tian, Z. Zhang, and Y. Wang, “Low-complexity optimization for two-dimensional direction-of-arrival estimation via decoupled atomic norm minimization,” in *Proc. Speech and Signal Processing (ICASSP) 2017 IEEE Int. Conf. Acoustics*, Mar. 2017, pp. 3071–3075.

[17] J. Cai, W. Xu, and Y. Yang, “Large scale 2D spectral compressed sensing in continuous domain,” in *Proc. Speech and Signal Processing (ICASSP) 2017 IEEE Int. Conf. Acoustics*, Mar. 2017, pp. 5905–5909.

[18] Z. Zhang, Y. Wang, and Z. Tian, “Efficient two-dimensional line spectrum estimation based on decoupled atomic norm minimization,” *Signal Processing*, vol. 163, pp. 95–106, Oct. 2019.

[19] Y. Wang, Y. Zhang, Z. Tian, G. Leus, and G. Zhang, “Angle-based channel estimation with arbitrary arrays,” in *Proc. IEEE Global Communications Conf. (GLOBECOM)*, Dec. 2019, pp. 1–6.

[20] ——, “Super-resolution channel estimation for arbitrary arrays in hybrid millimeter-wave massive MIMO systems,” *IEEE Journal of Selected Topics in Signal Processing*, vol. 13, no. 5, pp. 947–960, Sep. 2019.

[21] Z. Tian, Y. Tafesse, and B. M. Sadler, “Cyclic feature detection with sub-Nyquist sampling for wideband spectrum sensing,” *IEEE Journal of Selected Topics in Signal Processing*, vol. 6, no. 1, pp. 58–69, Feb. 2012.

[22] D. Romero, D. D. Ariananda, Z. Tian, and G. Leus, “Compressive covariance sensing: Structure-based compressive sensing beyond sparsity,” *IEEE signal processing magazine*, vol. 33, no. 1, pp. 78–93, 2015.

[23] Y. Zhang, G. Zhang, and X. Wang, “Computationally efficient doa estimation for monostatic mimo radar based on covariance matrix reconstruction,” *Electronics Letters*, vol. 53, no. 2, pp. 111–113, 2016.

[24] Z. Yang and L. Xie, “Enhancing sparsity and resolution via reweighted atomic norm minimization,” *IEEE Transactions on Signal Processing*, vol. 64, no. 4, pp. 995–1006, 2015.

[25] L. Vandenberghe and S. Boyd, “Semidefinite programming,” *SIAM review*, vol. 38, no. 1, pp. 49–95, 1996.

[26] S. Boyd, N. Parikh, E. Chu, B. Peleato, and J. Eckstein, *Distributed Optimization and Statistical Learning via the Alternating Direction Method of Multipliers*. now, 2011. [Online]. Available: https://ieeexplore.ieee.orghttps://ieeexplore.ieee.org/document/8186925

[27] H. Yan, J. Li, and G. Liao, “Multitarget identification and localization using bistatic mimo radar systems,” *EURASIP Journal on Advances in Signal Processing*, vol. 2008, pp. 1–8, 2007.

[28] M. Grant and S. Boyd, “CVX: Matlab software for disciplined convex programming, version 2.1,” http://cvxr.com/cvx, Mar. 2014.